Energy Management by means of SMD Model Analysis for AMB Systems with Eccentricity

Rupert Gouws

Abstract: This paper provides the spring-mass-damper (SMD) model analysis of a radial active magnetic bearing (AMB) system that displays eccentricity. Energy management of AMB systems can be done by means of a detailed SMD model analysis. It is specifically important to use SMD model analysis when the AMB system displays eccentricity. A SMD model analysis as well as the free-body diagram analysis is presented for the following scenarios: 1) rotational load unbalance, 2) foundation looseness, 3) rotating overhung rotor, 4) static eccentricity and 5) dynamic eccentricity.

Keywords: Active magnetic bearings, energy management, eccentricity, spring-mass-damper.

I. INTRODUCTION

Active magnetic bearing (AMB) systems represent modern mechatronical systems. These systems have advantages of high life time and low maintenance cost, due to the avoidance of lubricants and the absence of material deterioration and minimal friction losses [1], [2]. The use of AMB systems in motors, generators, pumps, turbo-machinery and compressors has increased over the last couple of years, since users expect that machines have high efficiency and high availability [3].

Energy management of AMB systems can be done by means of detailed spring-mass-damper (SMD) model analysis. It is specifically important to use SMD model analysis when the AMB system displays eccentricity. The SMD model also provides detail on the forces exerted on the AMB system, which can be further analyzed.

This paper provides the SMD model analysis of a radial AMB system that displays eccentricity. SMD model analysis as well as the free-body diagram analysis is presented for the following scenarios: 1) rotational load unbalance, 2) foundation looseness, 3) rotating overhung rotor, 4) static eccentricity and 5) dynamic eccentricity. More detail on the physical parameters of the radial AMB system is provided in reference [1]. The paper also presents the design of a real-time displacement analysis and correction system for vibration forces on rotor of rotational AMB system [1]. More detail on the impact of frequency switching on the efficiency of a fully suspended AMB system is presented in reference [3].

Rupert Gouws is with the North-West University, School of Electrical, Electronic and Computer Engineering, Potchefstroom, 2520, South Africa. Email: rupert.gouws@nwu.ac.za).

II. ROTATIONAL LOAD UNBALANCE

This section provides the SMD model analysis of a radial AMB system with rotational load unbalance. The radial AMB system with rotational load unbalance is shown in fig. 1.

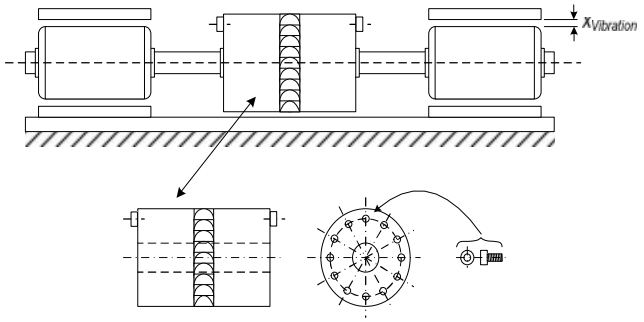

Fig. 1. Radial AMB system with rotational load unbalance.

Fig. 2 provides the free-body diagram for the AMB system with rotational load unbalance. One of the most common of vibration in engineering is rotating unbalance. This is where the rotating machine is not precisely balanced and the rotating out of balance mass causes forces on the engine.

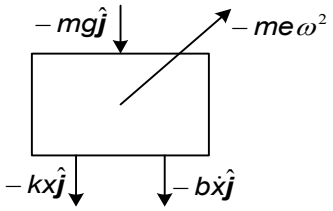

Fig. 2. Free-body diagram for the AMB system with rotational load unbalance.

Fig. 3 provides the SMD model for the AMB system with rotational load unbalance. We consider the complete engine (including the out of balance mass) to have mass M, and the unbalance mass itself to be m, rotating with eccentricity e.

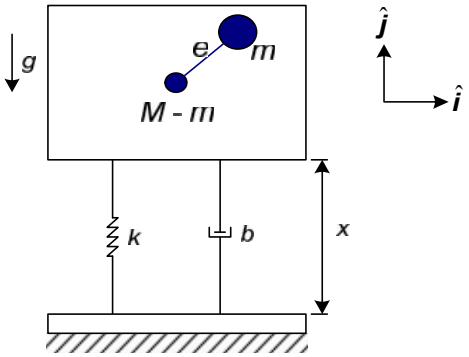

Fig. 3. Spring-Mass-Damper model for the AMB system with rotational load unbalance.

A real engine unbalance will cause vibration in at least two

planes (vertical and rocking), which can be simplified by exploring only pure vertical motion. The (vertical) displacement is measured from the equilibrium position, therefore:

Displacement of the non-rotating mass is given by:

$$(M - m) = x \tag{1}$$

Displacement of the rotating mass is given by:

$$m = x + e.sin(\omega t) \tag{2}$$

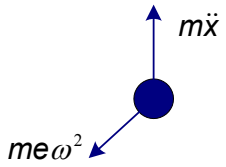

Fig. 4. Free-body diagram for the rotating mass

Fig. 4 provides the free-body diagram for the rotating mass. The resolved upward vertically forces are given by equation (3).

$$Tension_{VERTICALCOMPONENT} = m\ddot{x} - me\omega^2 \sin(\omega t) \tag{3}$$

The free-body diagram for the non-rotating mass is provided by fig. 3. The resolved upward vertically forces are given by equation (4).

$$Tension_{VERTICAL\,COMPONENT} - kx - c\dot{x} = (M - m)\ddot{x} \tag{4}$$

The equation of motion is given by equation (5).

$$-m\ddot{x} + me\omega^2 \sin(\omega t) - kx - c\dot{x} = (M - m)\ddot{x}$$

$$M\ddot{x} + c\dot{x} + kx = me\omega^2 \sin(\omega t) \tag{5}$$

The last equation is essentially the same as for force excitation, replacing the forcing function F_0 with ($me\omega^2$), which is a function of frequency. We can therefore write the dynamic response of the single degree of freedom with rotating unbalance by comparing the equation of motion with the force excitation case. The response is relative to the product "*me*".

$$\frac{X}{me} = \frac{\omega^2}{M\left\{\left(\omega_n^2 - \omega^2\right) + 2j\zeta\omega\omega_n\right\}} \tag{6}$$

The magnitude and phase of this complex function is given by equation (7) and equation (8).

$$\frac{X}{me} = \frac{\omega^2}{M\left\{\left(\omega_n^2 - \omega^2\right)^2 + 4\zeta^2\omega^2\omega_n^2\right\}^{1/2}} \tag{7}$$

and

$$\text{phase} = \tan^{-1}\left(\frac{2\zeta\omega\omega_n}{\omega_n^2 - \omega^2}\right) \tag{8}$$

Equation (5) can be written as follows:

$$\ddot{x} + \frac{c}{M}\dot{x} + \frac{k}{M}x = \frac{m}{M}e\omega^2 \sin(\omega t) \tag{9}$$

The standard form is given by equation (10).

$$\ddot{x} + 2\zeta\omega_n\dot{x} + \omega_n x = u_0 \sin(\omega t) \tag{10}$$

where

$$\omega_n = \sqrt{\frac{k}{M}} \text{ and } \zeta = \frac{c}{2\sqrt{kM}} \tag{11}$$

Equation (12) therefore provides the rotating unbalance with respect to the air-gap ($x(t)$).

$$x(t) = X\sin(\omega t - \varphi) \tag{12}$$

The parameter φ represents the phase shift of the unbalance force.

III. FOUNDATION LOOSENESS

This section provides the SMD model analysis of a radial AMB system with foundation looseness. Fig. 5 provides the radial AMB system with foundation looseness. More detail on the physical parameters of the radial AMB system is provided in reference [1].

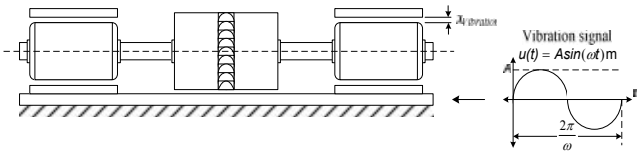

Fig. 5. Radial AMB system with foundation looseness.

Fig. 6 provides the free-body diagram for the AMB system with foundation looseness.

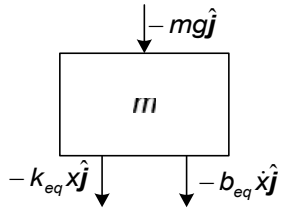

Fig. 6. Free-body diagram for the AMB system with foundation looseness.

Fig. 7 provides the SMD model for the AMB system with foundation looseness. The force F_d represent the vibration (disturbance) force occurring on the base of the AMB system. This vibration is usually referred to as foundation looseness. The force F_{ec} refers to the correction force applied onto the rotor in order to stabilize it.

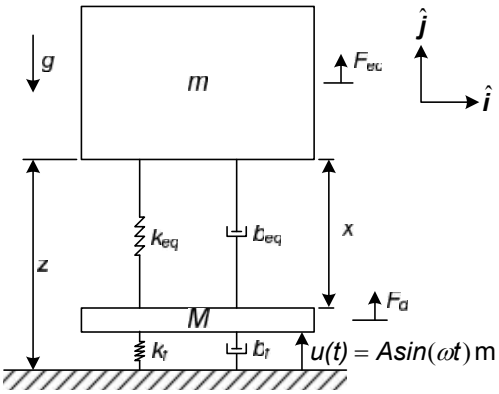

Fig. 7. Spring-Mass-Damper model for the AMB system with foundation looseness.

When a correction force F_{ec} is applied onto the AMB system, to cancel the effect of F_d, the forces on the parameters k_f and b_f increases. This may cause an increase in the stress of critical components, which may cause components to be damaged or break down. The components need to be identified by the user as critical or non-critical and the necessary steps must be taken to operate the AMB system under the fault condition or to shut down the AMB system and repair the fault.

The following calculations focus on forces acting on the mass m. We define the additional coordinate z, which measures the absolute displacement of the mass with respect to the ground, as:

$$z = x + u(t) \tag{13}$$

The free-body-diagram is shows in fig. 6. The only forces acting on the mass arise from the gravitational force, the spring force and the damping force. In terms of the identified coordinates, the acceleration of the mass center is given by equation (14).

$$^{\mathcal{F}}\boldsymbol{a}_G = \ddot{z}\,\hat{\boldsymbol{j}} = (\ddot{x} + \ddot{u})\,\hat{\boldsymbol{j}} \tag{14}$$

with

$$\ddot{u}(t) = -(u_0\omega^2)\sin(\omega t) \tag{15}$$

wherefore, the linear momentum balance on the mass yields:

$$\sum \boldsymbol{F} = m\,^{\mathcal{F}}\boldsymbol{a}_G \tag{16}$$

$$(-k_{eq}x - b_{eq}\dot{x} - mg)\,\hat{\boldsymbol{j}} = (m\ddot{x} + m\ddot{u})\,\hat{\boldsymbol{j}} \tag{17}$$

Writing this in terms of x, the equation of motion is given by equation (18).

$$m\ddot{x} + b_{eq}\dot{x} + k_{eq}x = -m\ddot{u}(t) - mg$$

$$\ddot{x} + \frac{b_{eq}}{m}\dot{x} + \frac{k_{eq}}{m}x = -\ddot{u}(t) - g \tag{18}$$

The standard form is given by equation (19).

$$\ddot{x} + 2\zeta\omega_n\dot{x} + \omega_n^2 x = u_0\omega^2\sin(\omega t) - g \tag{19}$$

with

$$\omega_n = \sqrt{\frac{k_{eq}}{m}} \quad \text{and} \quad \zeta = \frac{b_{eq}}{2\sqrt{km}} \tag{20}$$

The amplitude of the forcing is given by equation (21).

$$F = u_0\omega^2 = \frac{1}{2}\omega^2 \tag{21}$$

The steady state response of the system therefore becomes:

$$x(t) = A\sin(\omega t - \varphi) - g \tag{22}$$

where $x(t)$ is the air-gap and

$$A = u_0\Lambda(r,\zeta) \quad \text{and} \quad \tan\varphi = \frac{2\zeta r}{1 - r^2} \tag{23}$$

where

$$\Lambda = \frac{r^2}{\sqrt{(1-r^2)^2 + (2\zeta r)^2}} \quad \text{and} \quad r = \frac{\omega}{\omega_n} \tag{24}$$

IV. ROTATING OVERHUNG ROTOR

This section provides the SMD model analysis of a radial AMB system with a rotating overhung rotor. Fig. 8 provides the radial AMB system with a rotating overhung rotor.

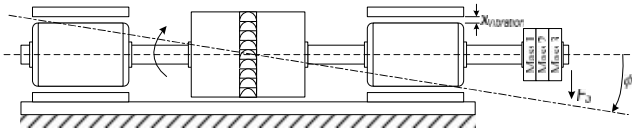

Fig. 8. Radial AMB system with a rotating overhung rotor.

Fig. 9 provides the free-body diagram for the AMB system with a rotating overhung rotor.

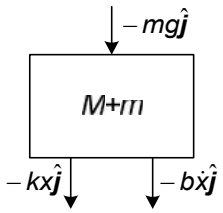

Fig. 9. Free-body diagram for the AMB system with a rotating overhung rotor.

Fig. 10 provides the SMD model for the AMB system with a rotating overhung rotor.

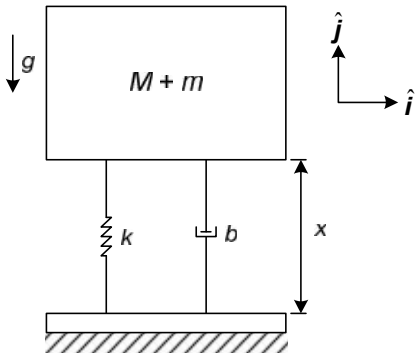

Fig. 10. Spring-Mass-Damper model for the AMB system with a rotating overhung rotor.

The resolved vertically forces can be written as follow:

$$(-kx - b\dot{x} - mg)\,\hat{\boldsymbol{j}} = (M + m)\ddot{x}\hat{\boldsymbol{j}} \tag{25}$$

The equation of motion is given by equation (26).

$$(M + m)\ddot{x} + b\dot{x} + kx = -mg \tag{26}$$

This can be written in the standard form as:

$$\ddot{x} + \frac{b}{M+m}\dot{x} + \frac{k}{M+m}x = \frac{-m}{M+m}g \tag{27}$$

where

$$\omega_n = \sqrt{\frac{k}{M+m}} \quad \text{and} \quad \zeta = \frac{b}{2\sqrt{k(M+m)}} \tag{28}$$

The air-gap ($x(t)$) function can therefore be written as follows:

$$x(t) = A\sin(\omega t - \varphi) - \frac{m}{M+m}g \tag{29}$$

More detail on a thermo-elasto-hydrodynamic model of the

Morton effect operating in overhung rotors supported by plain or tilting pad journal bearings is presented by [4].

V. STATIC ECCENTRICITY

This section provides the SMD model analysis of a radial AMB system with static eccentricity. Fig. 11 provides the radial AMB system with static eccentricity.

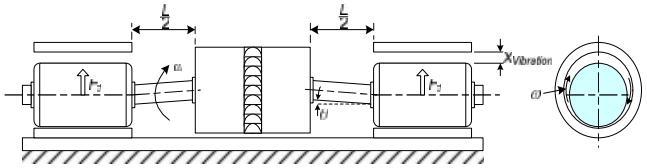

Fig. 11. Radial AMB system with static eccentricity.

Fig. 12 provides the free-body diagram for the AMB system with static eccentricity.

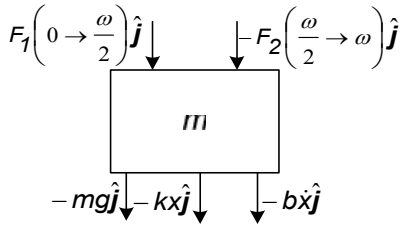

Fig. 12. Free-body diagram for the AMB system with static eccentricity.

Fig. 13 provides the SMD model for the AMB system with static eccentricity.

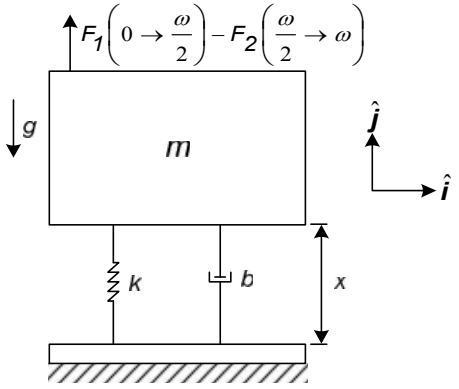

Fig. 13. Spring-Mass-Damper model for the AMB system with static eccentricity.

Static eccentricity (caused by the bent rotor interface) can be produced either by stator deformations or rotor axis displacement with respect to the stator axis. If the eccentricity is static, the air-gap function, x_{se}, can be approximated as follows:

$$x_{se}(\omega t, z) = x_0 - \delta(z)\cos(\omega t) \tag{30}$$

where $\delta(z)$ is the air-gap variation amplitude, which can vary along the axial length of the motor. The radial air-gap length under no eccentricity condition is given by x_0. As an example, if only one bearing is displaced respect to stator geometric axis, the air-gap variation amplitude can be approximated by equation (31).

$$\delta(z) = \delta_0 + kz \tag{31}$$

where δ_0 is the air-gap variation at $z = 0$, and k is a constant.

The inverse of the air-gap function can be approximated by equation (32).

$$x_{es}^{-1}(\omega t, z) = \frac{A_0(z)}{x_0} + \frac{A_1(z)}{x_0}\cos(\omega t) \tag{32}$$

where

$$A_0(z) = \frac{1}{\sqrt{1-\delta(z)}} \tag{33}$$

and

$$A_1(z) = 2\frac{1-\sqrt{1-\delta^2(z)}}{\delta(z)\sqrt{1-\delta^2(z)}} \tag{34}$$

Fundamental (first and second) natural frequency of the transverse vibration is given by equation (35).

$$f_{1,2} = C_1\sqrt{\frac{E_1 I_1 g_1}{W_1 L_1^4}} + C_2\sqrt{\frac{E_2 I_2 g_2}{W_2 L_2^4}} \tag{35}$$

As it was described in [5], there are two types of air-gap eccentricity, static and dynamic. Static eccentricity can be produced either by stator deformations or rotor axis displacement with respect to the stator axis. Due to that reason the air-gap is non-uniform, but remains constant for any rotor position.

Only the right half is evaluated, since the answer is the same for the other half only 180^o out of phase. Dynamic eccentricity occurs when the geometric center of the rotor is not at the center of rotation, producing a periodic variation in the air-gap when the rotor turns.

More detail on a method for dynamic simulation of air-gap eccentricity in induction machines is presented by [5].

VI. DYNAMIC ECCENTRICITY

This section provides the SMD model analysis of a radial AMB system with dynamic eccentricity. Fig. 14 provides the radial AMB system with dynamic eccentricity.

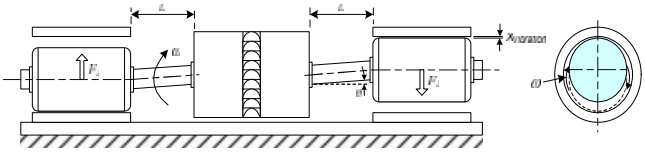

Fig. 14. Radial AMB system with dynamic eccentricity.

Fig. 15 provides the free-body diagram for the AMB system with dynamic eccentricity.

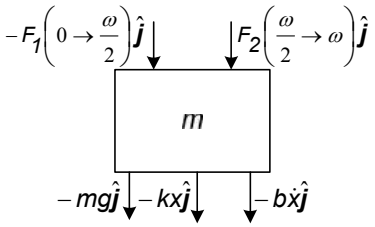

Fig. 15. Free-body diagram for the AMB system with dynamic eccentricity.

Fig. 16 provides the SMD model for the AMB system with dynamic eccentricity.

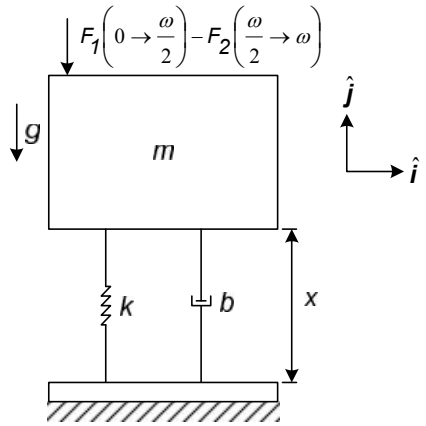

Fig. 16. Spring-Mass-Damper model for the AMB system with dynamic eccentricity.

If the eccentricity is dynamic, the air-gap function, x_{de}, can be approximated as follows:

$$x_{de}(\omega t, z, \varphi) = x_0 - \delta(z)\cos(\omega t - \varphi) \tag{36}$$

Fundamental (first and second) natural frequency of the transverse vibration is given by equation (37).

$$f_{1,2} = C_1\sqrt{\frac{E_1 I_1 g_1}{W_1 L_1^4}} + C_2\sqrt{\frac{E_2 I_2 g_2}{W_2 L_2^4}} \tag{37}$$

Vibration and misalignment greatly accelerate bearing wear and increase operating temperature.

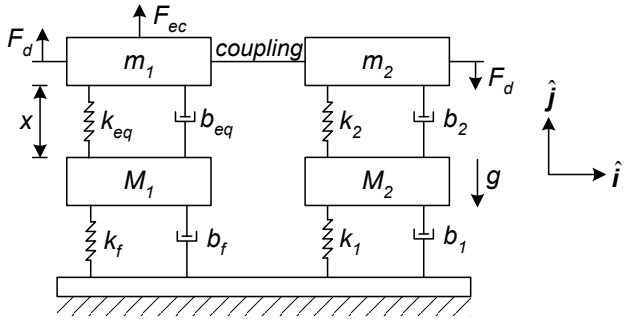

Fig. 17. Spring-mass-damper model for coupling misalignment

Fig. 17 shows the SMD model for coupling misalignment. In this figure the rotor of the magnetic bearing (with mass m_1) is driven by a motor unit (with mass m_2), which is not perfectly aligned. When the rotor starts turning a downwards force F_d starts acting on the rotor of the motor unit (m_2). The same force is propelled onto the rotor of the magnetic bearing (m_1). A correction force (F_{ec}) is applied onto the rotor to stabilise the rotor. The force on the coupling is therefore twice the force F_d. Although the effect of F_{ec} stabilises the rotor, it also increases stress on the coupling.

The magnetic bearing seems to be operating in good condition, but the motor unit (m_2) is under great stress. If both systems were AMBs, it would have been better to relax the reference displacement, therefore relieving stress on the motor unit (m_2).

More detail on combined effects of static and dynamic eccentricity on air-gap flux waves and the application of current monitoring to detect dynamic eccentricity in 3-phase induction motors is presented by [6].

VII. Conclusion

This paper presented the SMD model analysis of a radial AMB system that displays eccentricity. A SMD model analysis as well as the free-body diagram analysis is presented for the following scenarios: 1) rotational load unbalance, 2) foundation looseness, 3) rotating overhung rotor, 4) static eccentricity and 5) dynamic eccentricity.

It can be seen that it is important to use SMD model analysis when the AMB system displays eccentricity. SMD model analysis can also be used as an energy management tool to improve the energy consumption of the AMB system.

REFERENCES

[1] R. Gouws and G. van Schoor, "Real-time displacement analysis and correction system for vibration forces on rotor of rotational active magnetic bearing system," World Journal of Engineering, vol. 8, no. 4, pp. 381-394, 2011.

[2] G. Schweitzer, A. Traxler and H. Bleuler, "Magnetlager, grundlagen, eigenschaften und anwendungen berührungsfreier," Elektromagnetischer Lager, Springer Verlag, Berlin, 1993.

[3] R. Gouws, "Impact of frequency switching on the efficiency of a fully suspended active magnetic bearing system," International Journal of Physical Sciences vol. 7, no. 24, pp. 3073 - 3081, June 2012.

[4] A.C. Balbahadur, "A thermo-elasto-hydrodynamic model of the Morton effect operating in overhung rotors supported by plain or tilting pad journal bearings," Faculty of the Virginia Polytechnic Institute and State University, Blacksburg, Virginia, Feb. 2001.

[5] H. Toliyat, M. Areffen, and A. Parlos, "A method for dynamic simulation of air-gap eccentricity in induction machines," IEEE Transactions on Industry Applications, vol. 32, no. 4, pp. 910-918, Aug. 1996.

[6] D.G. Dorrell, W.T. Thomson, and S. Roach, "Combined effects of static and dynamic eccentricity on airgap flux waves and the application of current monitoring to detect dynamic eccentricity in 3-phase induction motors," Seventh International Conference on Electrical Machines and Drives, pp. 151-155, 1995.

Rupert Gouws holds a Ph.D. degree in Electrical and Electronic Engineering from the North-West University (Potchefstroom campus). He consulted to a variety of industry and public sectors in South Africa and other countries in the fields of energy engineering and engineering management. Currently he is appointed as a senior lecturer specialising in energy engineering, electrical machines and control at the North-West University. The Engineering Council of South Africa (ECSA) registered him as a Professional Engineer and the Association of Energy Engineers (AEE) certified him as a Certified Measurement and Verification Professional (CMVP).